

# Optimisation of the Measurement of the Arterial Input Function During High-Dose Administration for Dual Imaging Dynamic Contrast Enhanced (DCE) Magnetic Resonance Imaging (MRI) Applications in the Human Carotid Arteries

Philip M Robson<sup>1</sup>, Claudia Calcagno<sup>1</sup>, Sarayu Ramachandran<sup>1</sup>, Venkatesh Mani<sup>1</sup>, Melanie Kotys-Traugher<sup>2</sup>, and Zahi A Fayad<sup>1</sup>

<sup>1</sup>Translational and Molecular Imaging Institute, Mount Sinai School of Medicine, New York, NY, United States, <sup>2</sup>Philips Healthcare, Cleveland, OH, United States

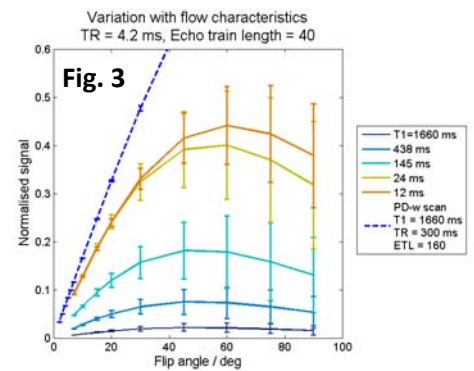
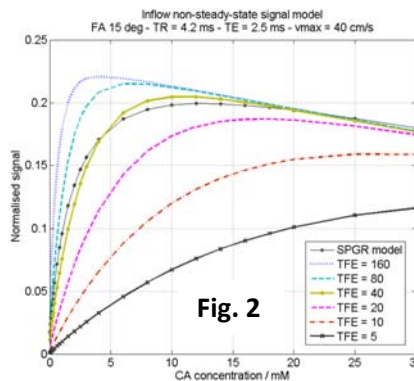
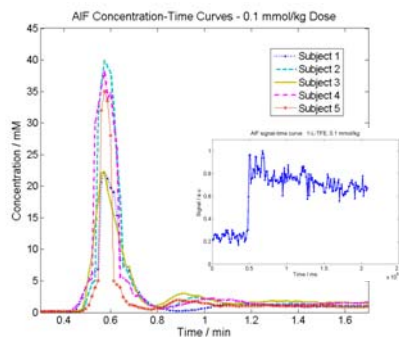
**Introduction:** Recently, Dynamic Contrast Enhanced (DCE) Magnetic Resonance Imaging (MRI) has gained interest in assessment of plaques in atherosclerosis in the carotid arteries (1,2). It is widely acknowledged that to measure the kinetic parameters accurately requires accurate measurement of the tissue uptake curve (Ct) and the arterial input function (AIF) (3). Current DCE-MRI methods extract Ct and AIF information from the same image data. This is sub-optimal for the carotid arteries where the vessel wall should be imaged with high spatial resolution, shows weaker signal enhancement than the vessel lumen, and requires slower temporal sampling than the first pass of the AIF. Dual imaging techniques (4-8) acquire the AIF and Ct data in separate images, acquired either separately in a dual-bolus approach, with a low-dose AIF scan preceding the high-dose tissue scan; or simultaneously, with one injection of the higher dose required for imaging uptake in the tissue.

Simultaneous dual imaging has potential advantages, namely, the elimination of ambiguity of CA dose scaling between the low dose test AIF bolus and high dose administered for the tissue-scan, temporal registration of AIF and Ct curves, and protocol simplicity; however, it poses specific problems: i) saturation of the signal recovery curve for very short T1 in a concentrated bolus; ii) inflow effects, and iii) signal modulation during non-steady-state 2D imaging required to maintain high temporal resolution of the AIF. To address these issues we propose acquiring short segments of saturation-prepared, radiofrequency-spoiled GRE, and present the results of a signal evolution model in the presence of inflow and signal modulation to convert signal to contrast-agent concentration.

**Methodology:** With written informed consent, in 5 subjects, DCE images were acquired successively with a 2D segmented rf-spoiled SPGR acquisition (FOV 160 mm, matrix 160x160, 2D slice perpendicular to the common carotid artery, TR=4.2 ms, TE=2.5 ms, FA=15°, echo-train-length 40, temporal resolution=0.8 sec, 3 T, Philips Achieva system) with a global saturation pulse preceding each segment, following injection of 0.1 mmol/kg dose of Gd-DTPA (Magnevist). Prior to CA administration, proton-density-weighted (PD-w) images were acquired to normalise DCE signal (same imaging parameters with TR=300 ms, FA=4°). AIF curves were measured as the average signal in ROIs on the carotid artery. In one subject an AIF was acquired with a single shot acquisition. AIF signal was converted to CA concentration using the signal-T1 relationship from our signal model. Magnetisation evolution was simulated for multiple T1 values with rotation by rf pulses at every TR, T1-recovery between excitations, decay due to T2\*≈T1, and inflow with a range of maximum velocities (50-900 mm/s) and velocity profiles (parabolic to plug flow) in the carotid arteries modelled as a cylinder, and assuming baseline blood T1 = 1660 ms. The average area under the modulation transfer function was recorded and the MTF was applied to the reconstruction of a synthetic carotid artery DCE image with the same acquisition FOV and resolution. To test the signal model used, in 3 cases, the area under the first pass bolus of the calculated concentration curves (I) was compared to the known dose (D) and cardiac plasma output (Q) according to I = D/Q (Hamilton dilution indicator). Cardiac output was measured with a standard 2D phase-contrast acquisition perpendicular to the ascending aorta, v<sub>enc</sub>=150 cm/s, retro-gated with 20 cardiac phases. The quantity I - D/Q was compared to a standard zero-mean distribution with the Student t-test.

**Results:** Measured AIF concentration-time curves are shown in Fig. 1. An AIF with single shot acquisition (insert) shows no discernible bolus peak and is deemed unsuitable for DCE measurements, clearly demonstrating the benefit of segmented acquisition. Signal to CA concentration curves from the signal model are shown in Fig. 2 for various segmentation strategies, with the conventional SPGR model for comparison. Fig. 3 shows the variability of signal in the model with changing maximum blood flow speed and flow profile, indicating low flip angles are preferable; additionally, linearity with flip angle of both DCE and PD-w signals indicates immunity of the signal measurements to B1 inhomogeneity. Quantification of measured AUC and known dose and cardiac output are shown in the Table; the p-value of 0.52 indicates no significant difference between the population of AIF concentration measurements and independent bolus dose-concentration estimates. Variance of 26% in the measured AUC is reasonable but could be improved.

Signal modeling indicates that even shorter segments may be required to prevent non-monotonic signal behaviour up to 30 mM which may be appropriate for full dose administration. In conclusion, measurement of the AIF in the carotid arteries with a full 0.1 mmol/kg dose can be achieved using a segmented SPGR acquisition and CA concentration can be calculated using a signal model accounting for inflow and non-steady-state signal recovery. With this approach, future investigation of simultaneous dual imaging techniques should be pursued.



	I / mM.min	(D/Q) / mM.min		(I - D/Q) / mM.min
1	2.73	3.53		-0.80
2	3.65	3.16		0.49
3	2.85	3.20		-0.35
4	4.27	-	Mean ± SD	-0.22 ± 0.6
5	2.21	-	p	0.52
Mean ± SD	3.14 ± 0.8	3.29 ± 0.2		

**References:** 1) Calcagno et al., ATVB 2008;28(7):1311-1317; 2) Kerwin et al., Radiology 2006;241(2): 459-468; 3) Parker et al., 1996; Proc. ISMRM:p.1582; 4) Calcagno et al., 2011; Proc. ISMRM:p.3316; 5) Kim et al., JMRI 2006;23(1):81-86; 6) Jelescu et al. JMRI;33(6):1291-1300. 7) Gatehouse et al., JMRI 2004;20(1):39-45; 8) Wang et al., 2011; Proc.ISMRM:p.1234